Fracture Toughness of Superplastic Formed/Diffusion Bonded Interfaces

Y. Xiang, S. Wu, and D. Chen

(Submitted 19 June 2001)

The present paper is concerned with the interfacial fracture problem of bi-material interfaces of superplastic forming/diffusion bonding (SPF/DB) components. It has been known that the interfacial fracture toughness is a strong function of the mode mixture of crack tip, which is the most important characteristic of interfacial problems. Micromechanical models have been proposed to understand this trend of interfacial toughness curves, based on which a modified criterion for fracture under mixed-mode loading is advanced in this paper to predict phenomenological functional forms of toughness curves. On the ground of linear elastic fracture mechanics (LEFM), mode I and mode II interfacial fracture toughnesses of SPF/DB components formed under different processing conditions have been measured in this paper using the double cantilever beam (DCB) and end-notched flexure (ENF) specimens, respectively. It is found that, just as is the general trend of interfacial fracture toughness curves, the experimental results of mode II toughness values are much greater than those of mode I toughness values, and the fluctuation of mode II toughness values under different processing conditions is much greater than that of mode I toughness values. On the basis of the experimental results, the four basic parameters in the modified criterion are obtained and the interfacial toughness curve of Ti-50A/Ti-6Al-4V SPF/DB components is determined using the modified criterion for fracture under mixed-mode loading. Comparison between the results shows that the agreement between experiment and theory is excellent.

Keywords diffusion bonding, fracture toughness, interfacial fracture, superplastic forming, Ti-50A, Ti-6Al-4V

1. Introduction

For many advanced material systems such as SPF/DB components, structural ceramics, and metal matrix composites, interfacial fracture is common and may, in large part, determine a material's overall mechanical response. For these material systems, it is the low fracture toughness that limits their use in engineering and industrial applications. So, there is an urgent need to understand, quantify, and improve the toughness of these advanced material systems; this has received wide attention in recent years.[1,2]

A crack in an isotropic, homogeneous material tends to grow in opening mode, and hence, the fracture toughness can be characterized by a single parameter, mode I toughness, K_{IC}. However, owing to the stress and strain concentration, material mismatch, and technical bonding flaw in the interface, a crack lying on an interface often tends to grow along the interface. Because the crack grows under mixed-mode conditions, it is necessary to quantify interfacial fracture toughness as a function of mode mixture. Experimental data on most interfaces have indicated that interfacial toughness increases as the mode mixture increases. Micromechanical models have been proposed to understand the trend of toughness curves,[3] so it is feasible to rely on these models to predict phenomenological functional forms of toughness curves. A general criterion for fracture under mixed-mode loading has been advanced by Charalambides *et al.*[4] However, in order to reflect the trend of the toughness curve more precisely, the criterion is modified in this paper to describe the toughness curves, through which we can determine the toughness curve of specific interfaces through only a couple of experimental values.

The superplastic forming/diffusion bonding (SPF/DB) combined technique is an advanced processing technique widely used in industry. Just as in other bi-material systems, the interface of SPF/DB components always becomes the fracture source in practice, and the interfacial fracture is the most typical failure form of SPF/DB components.[5] In this paper, the linear elastic fracture mechanics (LEFM) is applied to characterize the fracture performance of the interfaces, based on which mode I and mode II interfacial toughnesses of SPF/DB components have been measured using a double cantilever beam (DCB) specimen and end-notched flexure (ENF) specimen, respectively. On the grounds of the modified fracture criterion and the experimental results, the interfacial fracture toughness curve of specific SPF/DB components has been determined, the result of which provides a good basis for the processing route design and interfacial fracture toughness improvement of SPF/DB components.

2. Interfacial Fracture Mechanics

2.1 Basic Principles

Figure 1 gives the generic configuration of an interface crack. Material 1 is above the interface and material 2 is below it.

Assuming that the two materials are linearly elastic, homoge-

Y. Xiang, S. Wu, and **D. Chen,** Northwestern Polytechnical University, College of Materials Science and Engineering, Xi'an 710072, China. Contact e-mail: xiangyb@263.net.

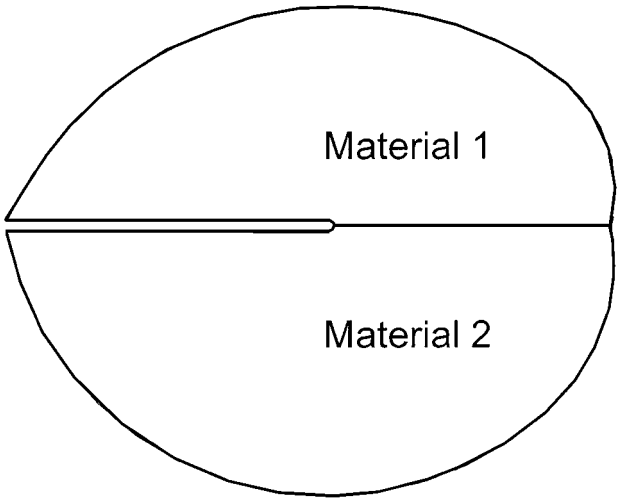

Fig. 1 Generic configuration of an interfacial crack

neous, and isotropic, the stress field is observed to depend only on two nondimensional Dundurs parameters:[6]

$$\alpha = \frac{\mu_1(\kappa_2 + 1) - \mu_2(\kappa_1 + 1)}{\mu_1(\kappa_2 + 1) + \mu_2(\kappa_1 + 1)}$$
$$\beta = \frac{\mu_1(\kappa_2 - 1) - \mu_2(\kappa_1 - 1)}{\mu_1(\kappa_2 + 1) + \mu_2(\kappa_1 + 1)} \quad \text{(Eq 1)}$$

and a related parameter

$$\varepsilon = \frac{1}{2\pi} \ln \frac{1 - \beta}{1 + \beta} \quad \text{(Eq 2)}$$

In the above expressions, μ is the shear modulus; κ is a nondimensional parameter related to Poisson's ratio ν ($\kappa = (3 - \nu)/(1 + \nu)$ for plane stress, and $\kappa = 3 - 4\nu$ for plane strain); the subscripts 1 and 2 refer to the two materials, respectively; and ε is the oscillatory index responsible for various pathological behaviors in linear elasticity solutions for interfacial cracks.

Attempts to analyze the above problem have led to considerable difficulties.[7] First, in order to satisfy the boundary conditions along the interface, a singularity of complex form was necessary,[8] resulting in the stresses oscillating with increasing frequency as the crack tip is approached. Second, the crack face displacements overlapped, resulting in a physically unreasonable situation. Third, the lack of an $r^{-1/2}$ singularity rendered the use of stress intensity factors problematic. However, the interlayer model advanced by Atkinson[9] and Yang[10] provides insightful interpretations of several important concepts of interface fracture mechanics, and thus, stress oscillation and displacement overlap are avoided successfully. In the interlayer model, a nonhomogeneous interlayer is introduced between two dissimilar materials to characterize the transition of the elastic modulus across the bi-material interface, the $r^{-1/2}$ singularity field near the tip of an advancing interlayer crack is related to the remote interface crack tip field, and also an approximate but explicit relation for the phase shift between the near tip and the remote singularity fields is derived. Using the interlayer model, the fracture can be expressed in terms of two parameters. The first parameter is the mode mixture ψ_{tip}, which is the phase angle of the relative proportion of the opening and sliding tractions ahead of the crack tip. The second parameter is the fracture toughness G, which can be evaluated based on the energy release rate at the onset of crack growth.

2.2 The Crack Mode Mixture

One important feature of bi-material interface cracks that should be emphasized is that ψ_{tip} is often nonzero, even when the external loading is normal to the interface plane.[11] This situation arises because of the elastic mismatch across the interface. When an interface fracture configuration is used to test interfacial fracture toughness, the crack always lies on the interlayer of the two-bonded material. Now, the strain energy release rate can be evaluated by testing the fracture energy at the onset of crack growth. However, the phase angle ψ_{tip} for the near tip stress field is modified from that of the asymptotic field. It has been shown that the modified phase angle can be related to the remote quantity through the following equation:[1]

$$\psi_{tip} = \psi + \varepsilon \ln h + \omega(\alpha, \beta) \quad \text{(Eq 3)}$$

Here, h represents the thickness of the interlayer of the bi-material, which can be measured by experiment. The phase shift angle ω here represents the material-related phase shift from the remote field to the near tip field, which is treated as a function of the Dundurs parameters α and β defined in Eq 1. A method to estimate the phase shift ω is detailed in Ref 10.

2.3 Energy Release Rate

A well-documented experimental fact is that the fracture toughness of an interface depends strongly on mode mixture. Therefore, it is fracture toughness values at various mode mixtures that fully characterize the fracture resistance of the interface. The fracture toughness curve $G(\psi_{tip})$ thus becomes a very important property of the bi-material interface. With the interfacial fracture toughness curve, it is easy to examine the fracture characteristics of specific bi-material interfaces in detail and to obtain the corresponding toughness values of a specific mode mixture at one's pleasure. Also, from the interfacial fracture toughness curve, some useful information can be obtained to help improve the fracture toughness of the components.

A typical interfacial fracture toughness curve is shown in Fig. 2, from where we can see that G increases as ψ_{tip} increases, especially when the crack opening becomes small, in which case there is a steep increase. These trends have been found to be attributed to crack shielding caused by roughness of the interface fracture surface and material nonlinearity.[12]

3. Modified Criterion for Mixed-Mode Failure

By analyzing numerical data presented in the literature, a general criterion for fracture under mixed-mode loading is proposed in Ref 4, which assumes that a crack loaded globally

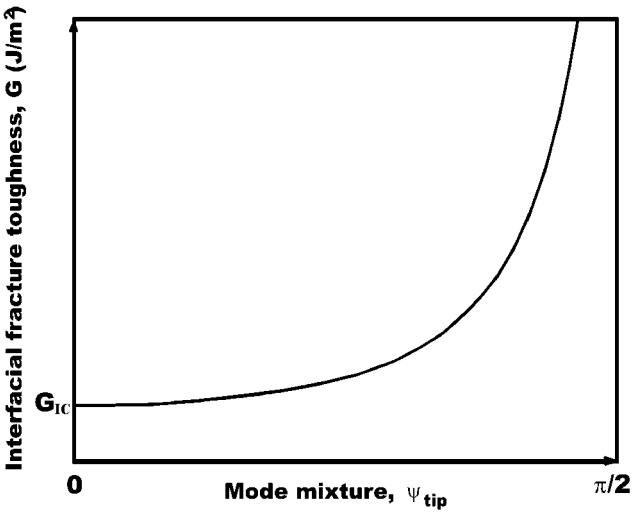

Fig. 2 Typical trend of the interfacial fracture toughness curve

with G_I and G_{II} will have an induced mode I component equal to the failure value, termed G_0, such that

$$G_0 = G_C[\cos^2(\psi_{tip} - \psi_0) + \sin^2\theta \sin^2(\psi_{tip} - \psi_0)] \quad \text{(Eq 4)}$$

where G_C is the measured fracture energy, ψ_{tip} is the mode mixture of the fracture tip, ψ_0 is the phase angle that arises from elastic mismatch across the bi-material interface, and θ can be regarded as the slope of the fracture surface roughness.

In Ref 4, the experimental validity of the mixed-mode failure criterion is successfully obtained by examining experimental results on crack propagation at bi-material interfaces from the literature. However, the interfacial toughness curve described by Eq. 4 is a little different from the real trend illustrated in Fig. 2, which lies in the fact that the increase of toughness slows down in the criterion, while the steep increase of toughness continues, in practice, when the crack opening becomes quietly small. A modification method is to introduce parameter λ into the trigonometric function to ensure the steep increase extent of the toughness. Thus, the general criterion for fracture under mixed-mode loading becomes

$$G_0 = G_C\{\cos^2[\lambda(\psi_{tip} - \psi_0)] + \sin^2\theta \sin^2[\lambda(\psi_{tip} - \psi_0)]\} \quad \text{(Eq 5)}$$

Here, if $\lambda = 1$, then Eq 5 reverts to Eq 4, from where the experimental validity of Eq 5 can also be obtained.

4. Experimental Procedure and Data Reduction

Because the toughness curve represents the fracture characteristics, it is significant to evaluate the interfacial fracture toughness curve $G(\psi_{tip})$ for specific bi-material interfaces. Using the above criterion for fracture under mixed-mode loading and Eq 5, the fracture toughness curve of specific bi-material

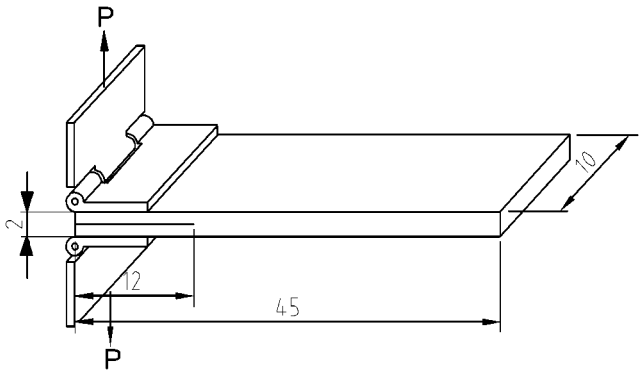

Fig. 3 DCB specimen dimensions (mm)

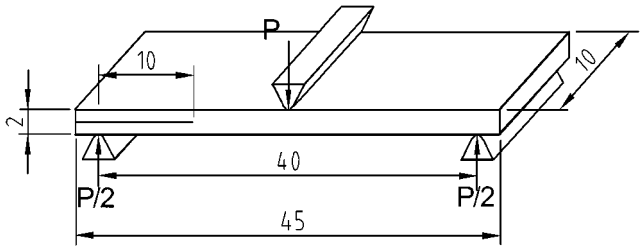

Fig. 4 ENF test specimen dimensions (mm)

interfaces can be determined. However, in order to deduce the four basic parameters in the model (*i.e.*, G_0, ψ_0, θ, and λ), we acquired a couple of experimental observations.

In this paper, mode I and mode II interfacial fracture toughnesses of specific SPF/DB components manufactured under different processing conditions have been measured using DCB and ENF tests, respectively. The materials used here are Ti-50A and Ti-6Al-4V sheets. Under different SPF/DB conditions, the two sheets are bonded together. A certain dope is laid on the specific place to avoid bonding, and thus, a natural crack is prefabricated in the midplane of the specimen. After SPF/DB deformation, DCB specimens and ENF specimens shown in Fig. 3 and 4 are cut from the SPF/DB components to perform the experiments.

Because of the different processing conditions of SPF/DB processes, different thicknesses of the specimen have been formed. Also, from the literature, it is known that, no matter what load is exerted on the specimen, mixed-mode loads will be induced at crack tips of bi-material interfaces.[7,8] The mismatch of material properties here results in shear stresses being induced by tensile stresses, and *vice versa*. Thus, based on the different thicknesses of the specimen measured, different mode mixtures of the specimen can be obtained from Eq 3. The thickness values here are measured under microscope and ten-point thickness values are averaged to obtain the final thickness value.

Also, using the DCB and ENF specimens, respectively, the fracture toughnesses of mode I and mode II can be measured with regard to the mode mixture of the crack tip.

4.1 Mode I Testing

For mode I testing, the hinged end tabs are glued onto the surface of the specimen for application of the load on the

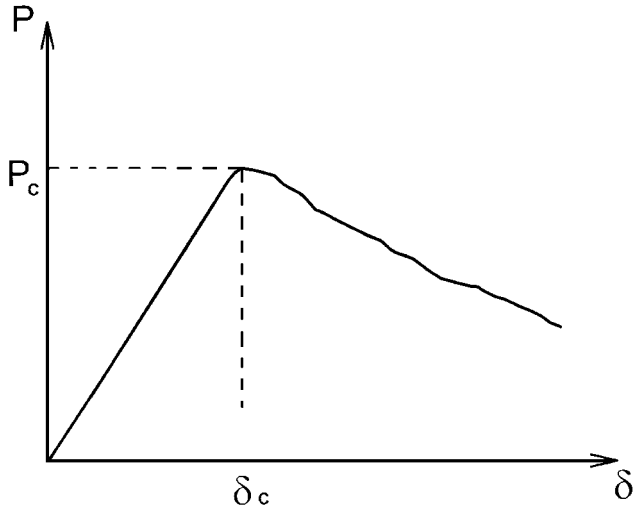

Fig. 5 Typical load-deflection curve of DCB testing

specimen during testing. The detailed geometry of the specimen is shown in Fig. 3. The test specimens are loaded in an Instron testing machine at a crosshead speed of 1 mm/min. An X-Y plotter is attached to the Instron machine to record the load-deflection response during the entire process. A typical load-deflection response is shown in Fig. 5.

From load, displacement, and crack length, the strain energy release rate (G_{IC}) may be calculated by using the general formula from LEFM:[13]

$$G_{IC} = \frac{P_C^2}{2B}\frac{\partial C}{\partial a} \qquad \text{(Eq 6)}$$

where P_C is the critical load at which the crack grows, a is the initial crack length, B is the width of the specimens, and C is the compliance, which is determined by the following equation:

$$C = \frac{\delta}{P} \qquad \text{(Eq 7)}$$

where δ is the corresponding deflection of load P.

Because the DCB specimen can be considered as a pair of cantilevers jointed at the crack tip, according to simple beam theory, the compliance can be expressed as follows:

$$C = \frac{2a^3}{3EI} = \frac{8a^3}{BEH^3} \qquad \text{(Eq 8)}$$

where E is the flexural modulus, $I = Bh^3/12$ is the second moment of cross-sectional area, and H is the half-thickness of the DCB specimen. Substituting Eq 8 into Eq 6, and expressing it in deflection form, we have

$$G_{IC} = \frac{3P_C\delta_C}{2Ba} \qquad \text{(Eq 9)}$$

where δ_C and P_C are the critical displacement and load, respectively.

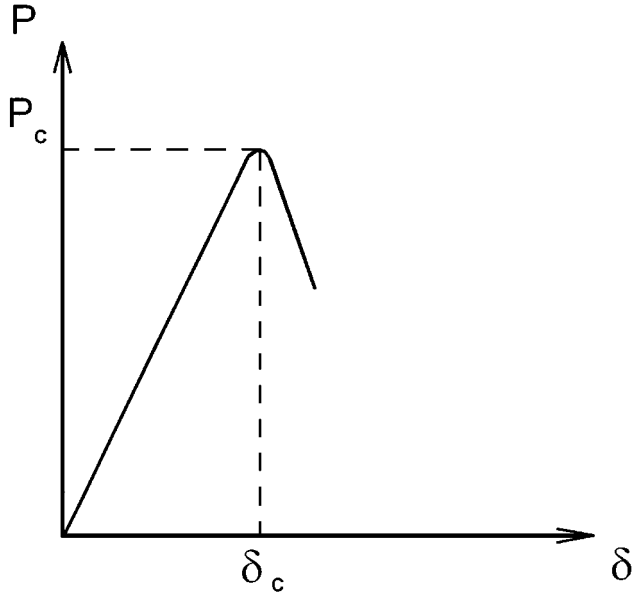

Fig. 6 Typical load-displacement curve of ENF testing

However, Eq 9 is only valid for the ideal conditions assumed in the beam theory, and corrections are necessary for large displacements, shear deformation, and rotation at the crack tip.[10] The usual method is to correct the crack length a into $a + \Delta$. The value of Δ may be found by plotting the cube root of compliance against the crack length. This gives an approximately straight line, which intersects the crack length axis at Δ. Thus, the critical strain-energy release G_{IC} now becomes

$$G_{IC} = \frac{3P_C\delta_C}{2B(a + \Delta)} \qquad \text{(Eq 10)}$$

4.2 Mode II Testing

The ENF fracture test is used to measure mode II delamination resistance. This is a three-point bend test in which the specimen contains a precrack, as shown in Fig. 4. The specimen is placed in such a way that the crack tip is midway between the loading roller and the outer support. The load is applied as controlled displacement (displacement rate 3 mm/min), and the crack growth is unstable in all cases. During the experiment, the curve of load against centerline deflection is recorded (Fig. 6). When the crack starts growing, a sudden load drop is observed and the test is stopped. The maximum recorded load and corresponding displacement are used in the data reduction process. Simple beam theory allows the calculation of the compliance, C, and, upon inserting this in Eq 6, the critical strain energy release rate can be calculated as[14]

$$G_{IIC} = 9a^2P_C\delta_C/2B(2L^3 + 3a^3) \qquad \text{(Eq 11)}$$

where L is the half-span and δ_C is the critical displacement.

Table 1 Interfacial fracture toughness and the corresponding tip mode mixture of different specimens

	Mode I		Mode II	
No.	ψ_{tip}	G_C (kJ/m^2)	ψ_{tip}	G_C (kJ/m^2)
A	−9.12°	1.14	75.98°	13.47
B	−6.58°	1.18	78.53°	15.99
C	−5.99°	1.20	79.12°	17.60
D	−5.18°	1.26	79.93°	18.17

Table 2 The four basic parameters in Eq 5 determined in the experiment

G_0	ψ_0	θ	λ
1.147	−12.6°	7.38°	0.84

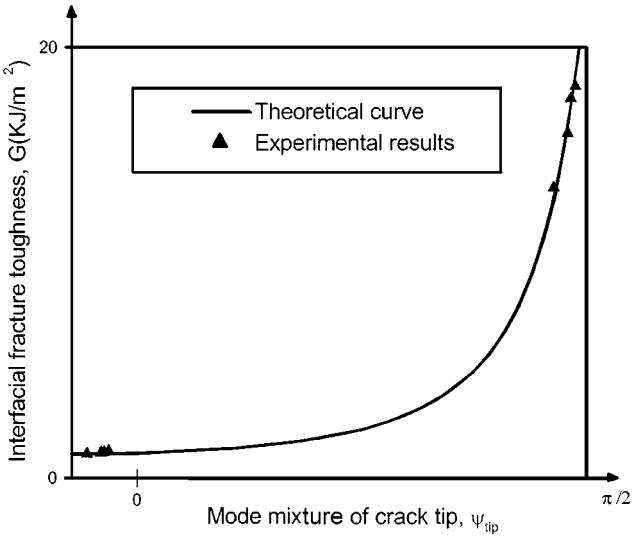

Fig. 7 Experimental and theoretical results of interfacial fracture toughness with respect to the mode mixture of crack tip

5. Results and Discussion

The results of mode I and mode II interfacial fracture toughness and the corresponding mode mixture of the crack tip for Ti-50A/Ti-6Al-4V SPF/DB components under different conditions are listed in Table 1.

It is obvious that mode II toughness values are much greater than mode I toughness values, and the fluctuation of mode II fracture toughness values under different processing conditions is much larger than that of mode I fracture toughness values, which is just the appropriate case in coincidence with the trend of the general interfacial fracture toughness curve (Fig. 2). According to Eq 5 and the experimental values, the interfacial fracture toughness curve of this material can be fitted and the four basic parameters can be determined, the result of which is listed in Table 2.

Figure 7 shows the comparison of experimental and theoretical results of the interfacial fracture toughness of Ti-50A/Ti-6Al-4V bi-material, from where it is seen that the agreement between experiment and theory is excellent. The line in Fig. 7 is the theoretical prediction of the interfacial fracture toughness curve, which can be expressed by the following equation:

$$G_c = 1.147/\{\cos^2[0.84(\psi_{tip} + 12.6)] + 0.0165 \sin^2[0.84(\psi_{tip} + 12.6)] \quad \text{(Eq 12)}$$

6. Conclusions

The present paper was concerned with the fracture problem of bi-material interfaces, especially when such failure occurs along the weak bi-material interfaces of SPF/DB components. In these cases, the interfacial fracture toughness curves, which fully characterize the fracture resistance of specific interfaces, should be taken into account when analyzing the fracture of such components and attempting to estimate the service life of engineering structures manufactured from such components. On the basis of the above results, the following conclusions may be drawn.

- The fracture toughness curve $G(\psi)$ is the most important property of bi-material interfaces. In general, G values increase as ψ increases; especially when the crack opening becomes small, there is a steep increase. These trends might be attributed to crack shielding caused by roughness of the interface fracture surface and material nonlinearity.
- Considering that the general criterion for fracture under mixed-mode loading advanced by Charalambides *et al.*[4] could not exactly reflect the situation during which the increase of toughness continues rising when the crack opening becomes quietly small. A modification method is advanced, and the modified criterion for fracture under mixed-mode loading is proposed in this paper as

$$G_0 = G_C\{\cos^2[\lambda(\psi_{tip} - \psi_0)] + \sin^2\theta \sin^2[\lambda(\psi_{tip} - \psi_0)]\}$$

- which can embody the trend of interfacial toughness curves more correctly. Here, G_C is the measured fracture energy, ψ_{tip} is the mode mixture of the fracture tip, ψ_0 is the phase angle that arises from elastic mismatch across the bi-material interface, λ is a parameter introduced into trigonometric functions, and θ can be regarded as the slope of the fracture surface roughness.
- The experimental results of mode II toughness values are much greater than those of mode I toughness values, and the fluctuation of mode II fracture toughness values under different conditions is much larger than that of mode I fracture toughness values, which is consistent with the trend of interfacial fracture toughness curves.

- On the basis of the experimental results, the four basic parameters in the modified criterion are obtained, and the interfacial toughness curve of Ti-50A/Ti-6Al-4V SPF/DB components is determined using the modified criterion for fracture under mixed-mode loading. Comparison between the results shows that the agreement between experiment and theory is excellent.

Acknowledgments

This work was mainly carried out at the College of Materials Science and Engineering, Northwestern Polytechnical University (Xi'an, People's Republic of China), with the financial support of the Research Fund for the Doctoral Program of Higher Education (Grant No. 98069912). Helpful discussions with Professors Li Miaoquan and Fu Zengxiang are gratefully acknowledged. The authors also thank the Aeronautical Manufacturing Institute of China and the Xi'an Aircraft Company for their experimental support of this paper.

References

1. Z. Suo and J.W. Hutchinson: *Mater. Sci. Eng. A*, 1989, vol. 107, pp. 135-43.
2. A.G. Evans, M. Ruhle, B.J. Dalgleish, and P.G. Charalambides: *Mater. Sci. Eng. A*, 1990, vol. 126, pp. 53-64.
3. A.G. Evans and J.W. Hutchinson: *Acta Met.*, 1989, vol. 37, p. 909.
4. M. Charalambides, A.J. Kinloch, Y. Wang, and J.G. Williams: *Int. J. Fracture*, 1992, vol. 54, pp. 269-91.
5. Wu Shichun: *Superplastic Deformation Theory of Metals*, National Defense Industry Press, Beijing, 1997 (in Chinese).
6. J. Dundurs: *J. Appl. Mech.*, 1969, vol. 36, pp. 650-52.
7. J.G. Williams: *Fracture Mechanics of Polymers*, Ellls Horwood, Wiley, Chichester, 1984, p. 55.
8. M.L. Williams: *Bull. Seismological Soc. America*, 1959, vol. 49, pp. 199-204.
9. C. Atkinson: *Acta Mech.*, 1977, vol. 26, pp. 103-13.
10. W. Yang and C.F. Shih: *Int. J. Solids Structures*, 1994, vol. 31, pp. 985-1002.
11. J.R. Rice: *J. Appl. Mech.*, 1988, vol. 55, p. 98.
12. A.G. Evans and J.W. Hutchinson: *Acta Metall.*, 1989, vol. 37, pp. 909-16.
13. D. Broek: *Elementary Engineering Fracture Mechanics*, 4th ed., 1986.
14. A.J. Russell and K.N. Street: *Delamination and Debonding of Materials*, ASTM STP 876, ASTM, Philadelphia, PA, 1985, p. 349.